

# Perspectives for the study of charm in-medium quenching at the LHC with ALICE

Andrea Dainese (ALICE Collaboration)

*Università degli Studi di Padova, via Marzolo 8, 35131 Padova, Italy*

e-mail: andrea.dainese@pd.infn.it

14th February 2019

## Abstract

Charm mesons produced in nucleus–nucleus collisions are expected to be less attenuated (quenched) by the medium than hadrons containing only light quarks, since radiative energy loss of heavy quarks should be reduced by the ‘dead-cone’ effect. We start from a published energy-loss model to derive the quenching for D mesons at the LHC, introducing an approximation of the dead-cone effect and employing a Glauber-based description of the geometry of central Pb–Pb collisions to estimate the in-medium path lengths of c quarks. We show that the exclusive reconstruction of  $D^0 \rightarrow K^- \pi^+$  decays in ALICE allows to measure the nuclear modification factor of the D mesons transverse momentum distribution and the  $D/\text{charged hadrons}$  ratio and, thus, to investigate the energy loss of c quarks.

## 1 Introduction

The ALICE experiment [1] at the LHC will study nucleus–nucleus (AA) collisions at a centre-of-mass energy  $\sqrt{s_{\text{NN}}} = 5.5$  TeV (for Pb–Pb) per nucleon–nucleon (NN) pair in order to investigate the properties of QCD matter at energy densities of up to several hundred times the density of atomic nuclei. In these conditions a deconfined state of quarks and gluons is expected to be formed.

Hard partons and heavy quarks, abundantly produced at LHC energies in initial hard-scattering processes, are sensitive probes of the medium formed in the collision as they may lose energy by gluon bremsstrahlung while propagating through the medium [2, 3, 4, 5]. The attenuation (quenching) of

leading hadrons and jets observed at RHIC [6, 7, 8, 9] is thought to be due to such a mechanism. The large masses of the charm and beauty quarks make them qualitatively different probes, since, on well-established QCD grounds, in-medium energy loss of massive partons is expected to be significantly smaller than that of ‘massless’ partons (light quarks and gluons) [10]. Therefore, a comparative study of the attenuation of massless and massive probes is a promising tool to test the consistency of the interpretation of quenching effects as energy loss in a deconfined medium and to further investigate the properties (density) of such medium.

In the first part of this paper, we shortly summarize a widely used model of parton energy loss and we discuss how we apply it in our simulation. In the second part, we show that the exclusive reconstruction of  $D^0 \rightarrow K^- \pi^+$  decays with ALICE allows to carry out the mentioned comparative quenching studies by measuring:

- the *nuclear modification factor* of D mesons as a function of transverse momentum ( $p_t$ )

$$R_{AA}(p_t) \equiv \frac{dN_{AA}/dp_t/\text{binary NN collision}}{dN_{pp}/dp_t}, \quad (1)$$

which would be equal to 1 if the AA collision was a mere superposition of independent NN collisions, without nuclear or medium effects; in central Au–Au collisions at RHIC ( $\sqrt{s_{NN}} = 200$  GeV)  $R_{AA} \simeq 0.2$  for both  $\pi^0$  and charged hadrons in the range  $4 < p_t < 8$  GeV/c [6, 7, 8];

- the ratio of the nuclear modification factors of D mesons and of charged (non-charm) hadrons, as a function of  $p_t$ :

$$R_{D/h}(p_t) \equiv R_{AA}^D(p_t) / R_{AA}^h(p_t); \quad (2)$$

hereafter, this quantity is called *D/charged hadrons* (D/h) ratio.

## 2 Parton energy loss and the dead-cone effect for heavy quarks

In this work we use the quenching probabilities (or weights) calculated in Ref. [11] in the framework of the ‘BDMPS’ (Baier-Dokshitzer-Mueller-Peigné-Schiff) formalism [3], which we summarize in the following. The energy loss obtained with the quenching weights is presented in Section 3.

An energetic parton produced in a hard collision radiates a gluon with a probability proportional to its path length  $L$  in the dense medium. Then, the radiated gluon undergoes multiple scatterings in the medium, in a Brownian-like motion with mean free path  $\lambda$  which decreases as the density of the medium increases. The number of scatterings of the radiated gluon is also proportional to  $L$ . Therefore, the average energy loss of the parton is proportional to  $L^2$ .

The scale of the energy loss is set by the ‘maximum’ energy of the radiated gluons, which depends on  $L$  and on the properties of the medium:

$$\omega_c = \hat{q} L^2/2, \quad (3)$$

where  $\hat{q}$  is the transport coefficient of the medium, defined as the average transverse momentum squared transferred to the projectile per unit path length,  $\hat{q} = \langle q_t^2 \rangle_{\text{medium}} / \lambda$  [11].

In the case of a static medium, the distribution of the energy  $\omega$  of the radiated gluons (for  $\omega \ll \omega_c$ ) is of the form:

$$\omega \frac{dI}{d\omega} \simeq \frac{2\alpha_s C_R}{\pi} \sqrt{\frac{\omega_c}{2\omega}}, \quad (4)$$

where  $C_R$  is the QCD coupling factor (Casimir factor), equal to 4/3 for quark–gluon coupling and to 3 for gluon–gluon coupling. The integral of the energy distribution up to  $\omega_c$  estimates the average energy loss of the parton:

$$\langle \Delta E \rangle = \int_0^{\omega_c} \omega \frac{dI}{d\omega} d\omega \propto \alpha_s C_R \omega_c \propto \alpha_s C_R \hat{q} L^2. \quad (5)$$

The average energy loss is: proportional to  $\alpha_s C_R$  and, thus, larger by a factor  $9/4 = 2.25$  for gluons than for quarks; proportional to the transport coefficient of the medium; proportional to  $L^2$ ; independent of the parton initial energy  $E$ . It is a general feature of all parton energy loss calculations [2, 3, 4, 5, 11, 12] that the energy distribution (4) does not depend on  $E$ . Depending on how the kinematic bounds are taken into account, the resulting  $\Delta E$  is  $E$ -independent [3] or depends logarithmically on  $E$  [12]. However, there is always a stronger intrinsic dependence of the radiated energy on the initial energy, determined by the fact that the former cannot be larger than the latter,  $\Delta E \leq E$ . Within the above toy-model derivation which agrees with the main features of the BDMPS formalism, this kinematic constraint could be included by truncating the gluon energy distribution  $\omega dI/d\omega$  at  $\min(\omega_c, E)$  rather than at its natural upper limit  $\omega_c$ . This would give, from (4) and (5),  $\langle \Delta E \rangle \propto \alpha_s C_R \sqrt{\omega_c} \sqrt{\min(\omega_c, E)}$ . For

$E < \omega_c$ , we have  $\langle \Delta E \rangle \propto \sqrt{\hat{q}} \sqrt{E} L$ : the kinematic constraint turns the  $L$ -dependence from quadratic to linear. As we shall discuss in Section 3, the kinematic constraint can be equivalently interpreted as a reduction of the effective path length in the medium, i.e. of the length along which the energy of the parton is larger than zero and gluons can be radiated.

The transport coefficient is proportional to the density of the scattering centres and to the typical momentum transfer in the gluon scattering off these centres. A review of the estimates for the value of the transport coefficient in media of different densities can be found in Ref. [13]: the estimate is  $\hat{q}_{\text{cold}} \simeq 0.05 \text{ GeV}^2/\text{fm}$  for cold nuclear matter and up to  $0.5 \text{ GeV}^2/\text{fm}$  for a hadron gas; for a QGP formed at the LHC with energy density  $\epsilon \sim 50\text{--}100 \text{ GeV}/\text{fm}^3$ ,  $\hat{q}$  is expected to be of  $\simeq 5\text{--}10 \text{ GeV}^2/\text{fm}$ .

The medium-induced energy loss of heavy quarks was first studied in Refs. [14, 15]. Later, in Ref. [10] it was argued that for heavy quarks, because of their large mass, the radiative energy loss should be lower than for light quarks. The predicted consequence of this effect was an enhancement of the ratio of D mesons to pions (or hadrons in general) at moderately-large ( $5\text{--}10 \text{ GeV}/c$ ) transverse momenta, with respect to that observed in the absence of energy loss.

Heavy quarks with momenta up to  $40\text{--}50 \text{ GeV}/c$  propagate with a velocity which is significantly smaller than the velocity of light. As a consequence, in the vacuum, gluon radiation at angles  $\Theta$  smaller than the ratio of their mass to their energy  $\Theta_0 = m/E$  is suppressed by destructive quantum interference [16]. The relatively depopulated cone around the heavy-quark direction with  $\Theta < \Theta_0$  is called ‘dead cone’.

In Ref. [10] the dead-cone effect is assumed to characterize also in-medium gluon radiation and the energy distribution of the radiated gluons (4), for heavy quarks, is estimated to be suppressed by the factor:

$$\left. \frac{dI}{d\omega} \right|_{\text{Heavy}} / \left. \frac{dI}{d\omega} \right|_{\text{Light}} = \left[ 1 + \frac{\Theta_0^2}{\Theta^2} \right]^{-2} = \left[ 1 + \left( \frac{m}{E} \right)^2 \sqrt{\frac{\omega^3}{\hat{q}}} \right]^{-2} \equiv F_{\text{H/L}}, \quad (6)$$

where the expression for the characteristic gluon emission angle [10]  $\Theta \simeq (\hat{q}/\omega^3)^{1/4}$  has been used. The heavy-to-light suppression factor  $F_{\text{H/L}}$  in (6) increases (less suppression) as the heavy-quark energy  $E$  increases (the mass becomes negligible) and it decreases at large  $\omega$ , indicating that the high-energy part of the gluon radiation spectrum is drastically suppressed by the dead-cone effect.

The first (indirect) measurements of charm production, in the semi-electronic decay channel, in Au–Au collisions at RHIC [17] indicate (within the still large experimental errors) that there may be no attenuation of the D

meson  $p_t$  distribution, contrarily to what observed for pions and charged hadrons. This result supports the scenario proposed in Ref. [10] and it has stimulated considerable theoretical interest in the subject [18, 19]. Our approach, described in the next section, is to implement in the energy-loss simulation an algorithm to account for the dead-cone effect.

### 3 Simulation of energy loss

The quenching weight [20, 11] is defined as the probability that a hard parton radiates an energy  $\Delta E$  due to scattering in spatially-extended QCD matter. In Ref. [11], the weights are calculated on the basis of the BDMPS formalism, taking into account both the finite in-medium path length  $L$  and the dynamic expansion of the medium after the nucleus–nucleus collision. The input parameters for the calculation are the length  $L$ , the transport coefficient  $\hat{q}$  and the parton species (light quark or gluon).

The distribution of the in-medium path length in the plane transverse to the beam line<sup>1</sup> for central Pb–Pb collisions (impact parameter  $b < 3.5$  fm, corresponding to the 5% most central collisions) is calculated in the framework of the Glauber model for the collision geometry [21]. For a given impact parameter, hard-parton production points are sampled according to the density  $\rho_{\text{coll}}(x, y)$  of binary nucleon–nucleon collisions in the transverse plane and their azimuthal propagation directions are sampled uniformly. For a parton with production point  $(x_0, y_0)$  and azimuthal direction  $(u_x, u_y)$ , the path length is defined as:

$$L = \frac{\int_0^\infty dl l \rho_{\text{coll}}(x_0 + l u_x, y_0 + l u_y)}{0.5 \int_0^\infty dl \rho_{\text{coll}}(x_0 + l u_x, y_0 + l u_y)}. \quad (7)$$

Many sampling iterations are performed varying the impact parameter  $b$  from 0.25 fm to 3.25 fm in steps of 0.5 fm. The obtained distributions are given a weight  $b$ , since we verified that  $d\sigma^{\text{hard}}/db \propto b$  for  $b < 3.5$  fm, and summed. The result is shown in Fig. 1. The average length is 4.5 fm, corresponding to about 70% of the radius of a Pb nucleus and the distribution is significantly shifted towards low values of  $L$  because a large fraction of the partons are produced in the periphery of the superposition region of the two nuclei (‘corona’ effect).

The definition of  $L$  in (7) is exact in the case of a cylindrical collision density profile (i.e.  $\rho_{\text{coll}} = \rho_0 \Theta(R - \sqrt{x^2 + y^2})$  for a cylinder with radius  $R$ ). It is approximated for a realistic profile (derived from a Wood-Saxon nuclear density profile). The inclusion of nuclear geometry effects is not straight-forward

---

<sup>1</sup>Partons produced at central rapidities propagate in the transverse plane.

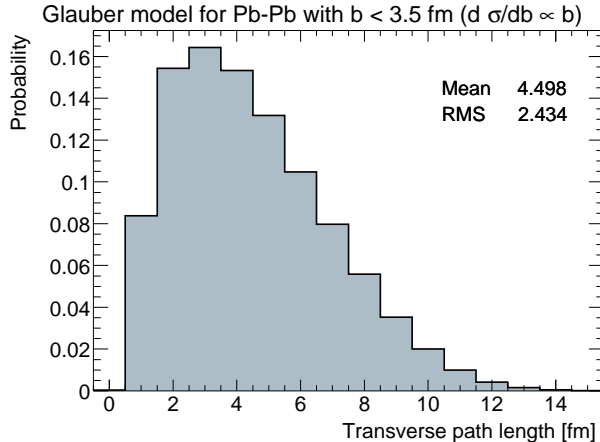


Figure 1: Distribution of the path lengths in the transverse plane for partons produced in Pb–Pb collisions with impact parameter  $b < 3.5$  fm.

in the scheme of the quenching weights, where the transport coefficient and the path length are considered as two distinct input parameters. Indeed, the lower medium density in the ‘corona’ could be modeled with a reduction of the transport coefficient or of the path length. However, since the energy loss is determined by the quantities  $\omega_c \propto \hat{q} L^2$  and  $\omega_c L \propto \hat{q} L^3$  [11], the optimal solution would be to include the geometry profile directly in the calculation of these two parameters, defining them as line integrals in  $dl$  similar to the integrals that appear in (7). For this work we adopt (7) as a practical definition of length in the medium, which allows us to employ a distribution of  $L$  rather than a constant value; in the following we show that this point is quite relevant. A more refined treatment of nuclear geometry is discussed in Ref. [22], where, however, energy loss is modeled as a simple exponential absorption that cannot be directly related to the medium properties.

For a given value of the transport coefficient  $\hat{q}$  and a given parton species, we use the numerical routine provided in Ref. [11] to calculate the energy-loss probability distribution  $P(\Delta E; L)$  for the integer values of  $L$  up to 15 fm. Then, these 15 distributions are weighted according to the path-length probability in Fig. 1 and summed up to obtain a global energy-loss probability distribution  $P(\Delta E)$ . The energy loss to be used for the quenching simulation can be directly sampled from the  $P(\Delta E)$  distribution corresponding to the chosen  $\hat{q}$  and to the correct parton species. Figure 2 (left) reports  $P(\Delta E)$  for light quarks and for gluons, as obtained with different values of the transport coefficient; in the figure, the ‘peak’ at  $\Delta E = 0$  represents the probability to have no medium-induced gluon radiation.

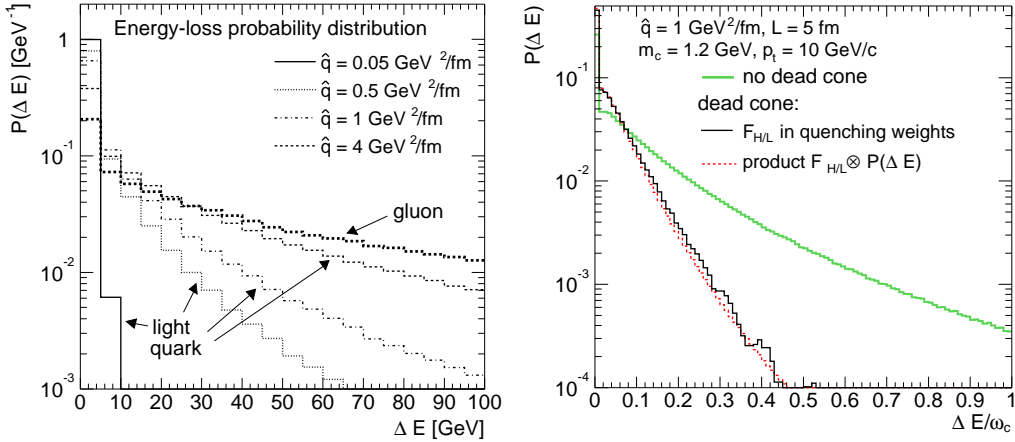


Figure 2: Left: energy-loss probability distribution,  $P(\Delta E)$ , for different values of  $\hat{q}$ , for light quarks and for gluons (thicker dashed line, only for 4 GeV<sup>2</sup>/fm). Right:  $P(\Delta E)$  for c quarks ( $m_c = 1.2$  GeV,  $p_t = 10$  GeV/c) without dead cone and with two different implementations of the dead-cone effect (see text).

The predicted lower energy loss for charm quarks is accounted for by multiplying the  $P(\Delta E)$  distribution for light quarks by the dead-cone suppression factor  $F_{H/L}(m, E, \hat{q}, \omega = \Delta E)$  given in (6). Since  $F_{H/L}$  depends on the heavy-quark energy  $E$ , the multiplication has to be done for each c quark or, more conveniently, in bins of the quark energy. It was verified that this multiplication is equivalent to recalculating the quenching weights with the gluon energy distribution for heavy quarks modified according to (6). The results on the energy-loss probability distribution obtained with the two methods, ‘ $F_{H/L} \otimes P(\Delta E)$  product’ and ‘ $F_{H/L}$  in the quenching weights’, were compared for  $\hat{q} = 1$  GeV<sup>2</sup>/fm,  $L = 5$  fm,  $m_c = 1.2$  GeV and  $p_t = 10, 20, 30$  GeV/c [28]. The comparison for  $p_t = 10$  GeV/c, shown in Fig. 2 (right), is quite satisfactory. A similar agreement is found for  $p_t = 20$  and 30 GeV/c.

Figure 3 shows the average relative energy loss as a function of the transverse momentum for gluons, light quarks and charm quarks ( $m_c = 1.2$  GeV). Different values of the transport coefficient  $\hat{q}$  are considered in the various panels and the described dead-cone correction (energy-dependent  $F_{H/L} \otimes P(\Delta E)$  product) is used for charm quarks. For each value of the parton  $p_t$  many values of  $\Delta E$  are sampled according to the energy-loss probability distribution and the kinematic constraint  $\Delta E \leq E$ , discussed in Section 2, is applied as follows: if  $\Delta E > p_t$ , then  $\Delta E = p_t$ . The ratio of the relative energy losses for gluons and for light quarks is compatible with the ratio of their

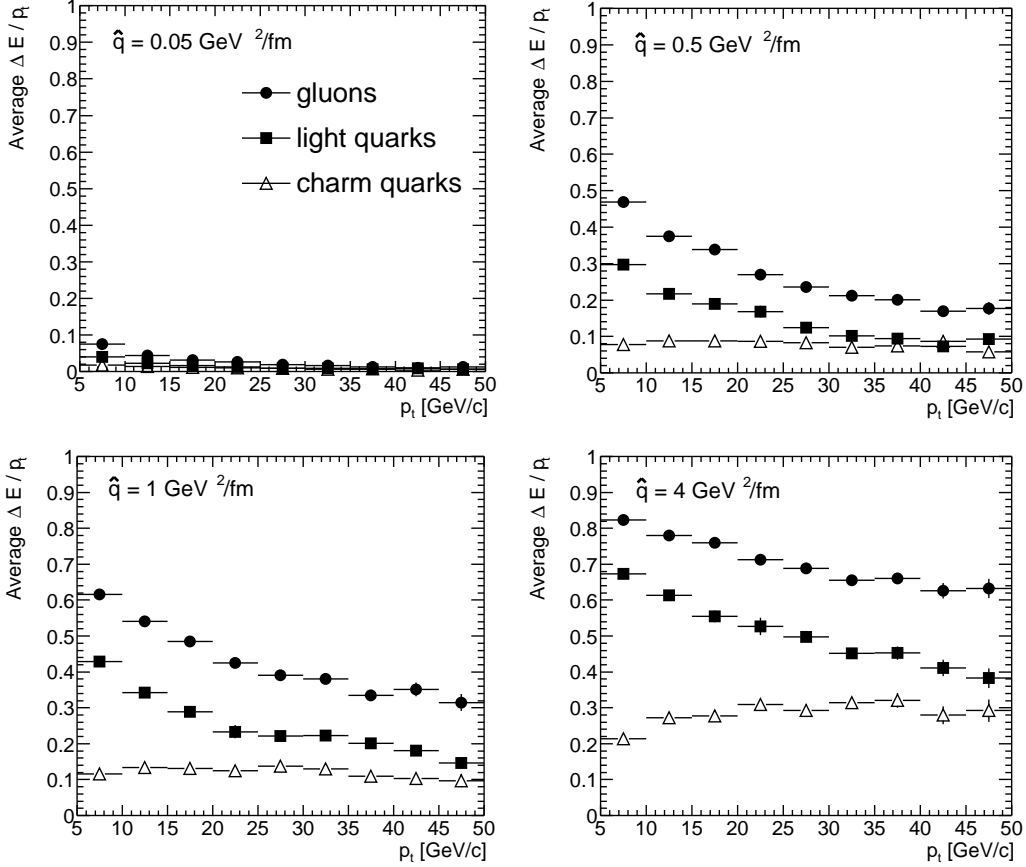


Figure 3: Average relative energy loss as function of the transverse momentum for gluons, light (massless) quarks and charm quarks ( $m_c = 1.2 \text{ GeV}$ ).

Casimir factors (2.25) at high  $p_t$ , where the kinematic constraint is not relevant. The ratio of the relative energy losses for light quarks and c quarks increases with increasing  $\hat{q}$ , particularly in the high- $p_t$  region, showing that the dead-cone effect is medium-dependent. With  $\hat{q} = 4 \text{ GeV}^2/\text{fm}$ , our estimated transport coefficient for the LHC (see next paragraph), the average relative energy loss is  $\approx (85 - 0.6 p_t(\text{GeV}/c))\%$  for gluons,  $\approx (75 - 0.8 p_t(\text{GeV}/c))\%$  for light quarks and  $\approx 25\text{--}30\%$  for c quarks.

Remarkably, for charm quarks we find that, for given  $\hat{q}$ , the average relative energy loss is approximately independent of the quark energy,  $\langle \Delta E/E \rangle \approx \text{const.}$ , (see Fig. 3), while for massless partons the average relative energy loss is clearly decreasing as the parton energy increases (the BDMPS average relative energy loss for massless partons would be  $\langle \Delta E/E \rangle \propto 1/E$ ;

this dependence is, then, weakened by the kinematic constraint). On the basis of this observation we expect that not only the magnitude but also the  $p_t$ -dependence of the nuclear modification factor  $R_{AA}$  of D mesons can be significantly affected by the dead cone.

Before describing the estimation of the transport coefficient to be used in the simulation, we shortly comment on the implementation of the kinematic constraint. Taking, as we do,  $\Delta E = p_t$  when the sampled  $\Delta E$  is larger than  $p_t$  is equivalent to truncating the energy-loss probability distribution  $P(\Delta E)$  at  $\Delta E = p_t$  and adding the  $\delta$ -function  $\delta(\Delta E - p_t) \int_{p_t}^{\infty} d\mathcal{E} P(\mathcal{E})$  to it. The total integral of  $P$  is, in this way, maintained equal to 1. The dependence of the final result on the kinematic constraint was argued [23, 11] to illustrate the theoretical uncertainties. These can be sizeable (more than a factor 2) for low  $p_t$  and sufficiently large  $\hat{q}$  and  $L$  in the present study. They should be improved in a refined calculation but we did not try to quantify them in detail<sup>2</sup>.

For the estimation of the transport coefficient  $\hat{q}$  we require for central nucleus–nucleus collisions at the LHC a leading-particle quenching at least of the same magnitude as that observed at RHIC. We, therefore, derive the nuclear modification factor  $R_{AA}$  for charged hadrons produced at the LHC and we choose the transport coefficient in order to obtain  $R_{AA} \simeq 0.2$ – $0.3$  in the range  $5 < p_t < 10$  GeV/ $c$  (for RHIC results see e.g. Refs. [6, 7, 8]).

The transverse momentum distributions, for  $p_t > 5$  GeV/ $c$ , of charged hadrons are generated by means of the chain:

1. generation of a parton, quark or gluon, with  $p_t > 5$  GeV/ $c$ , using PYTHIA [25] proton–proton with  $\sqrt{s} = 5.5$  TeV and CTEQ 4L parton distribution functions [26]; with these parameters, the parton composition given by PYTHIA is 78% gluons and 22% quarks (average over  $p_t > 5$  GeV/ $c$ );
2. sampling of an energy loss  $\Delta E$  according to  $P(\Delta E)$  and calculation of the new transverse momentum of the parton,  $p'_t = p_t - \Delta E$  (if  $\Delta E > p_t$ ,  $\Delta E = p_t$  and  $p'_t = 0$ );
3. (independent) fragmentation of the parton to a hadron using the leading-order Kniehl-Kramer-Pötter (KKP) fragmentation functions [27].

Quenched and unquenched  $p_t$  distributions are obtained including or excluding the second step of the chain. Figure 4 shows  $R_{AA}$  for hadrons, calculated

---

<sup>2</sup>These topics are considered also in Ref. [24] of which the author became aware while finalizing the present work. Very useful discussions with the authors of Ref. [24] are acknowledged.

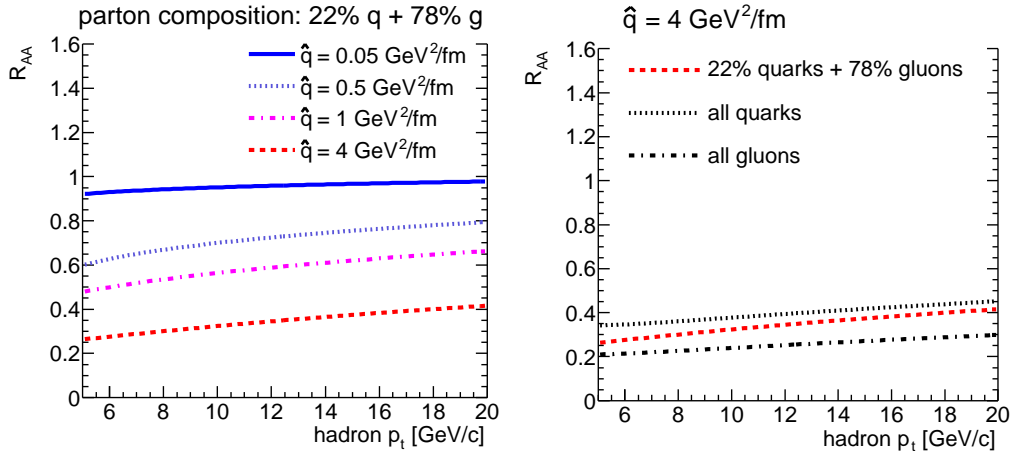


Figure 4: Nuclear modification factor for charged hadrons for different values of  $\hat{q}$  (left) and comparison of quark and gluon quenching for  $\hat{q} = 4$  GeV<sup>2</sup>/fm (right).

as the ratio of the  $p_t$  distribution with quenching to the  $p_t$  distribution without quenching. Different values of  $\hat{q}$  are considered in the left-hand panel of the figure: a value as large as 4 GeV<sup>2</sup>/fm is necessary to have  $R_{AA} \simeq 0.25$ –0.3 in  $5 < p_t < 10$  GeV/c. In the right-hand panel, for  $\hat{q} = 4$  GeV<sup>2</sup>/fm, we compare the results obtained considering all partons as gluons or all partons as quarks, in order to remark and quantify the larger quenching of gluons with respect to quarks.

Since the transport coefficient determines the size of the energy-loss effect, we shortly discuss the choice of  $\hat{q} = 4$  GeV<sup>2</sup>/fm. This value corresponds, according to the estimates reported in Ref. [13], to an energy density  $\epsilon \simeq 40$ –50 GeV/fm<sup>3</sup>, which is about a factor 2 lower than the maximum energy density expected for central Pb–Pb collisions at the LHC. The value is, therefore, reasonable.

Using the same quenching weights, the suppression observed at RHIC is reproduced in Ref. [11] with the much lower value  $\hat{q} = 0.75$  GeV<sup>2</sup>/fm. However, the constant length  $L = 6$  fm is there used, rather than a realistic distribution of lengths, thus obtaining a significantly stronger quenching. This simple approximation captures the main features of  $R_{AA}$  for 5–10% central collisions, which depend on the combination  $\hat{q} L^3$  ( $\propto \omega_e L$ ) more than on  $\hat{q}$  and  $L$  separately [11]. In addition, transverse momentum distributions are steeper at RHIC energy than at LHC energy and, consequently, to obtain the same  $R_{AA}$  suppression in the two cases one needs a larger  $\hat{q}$  (or  $\langle \Delta E \rangle$ )

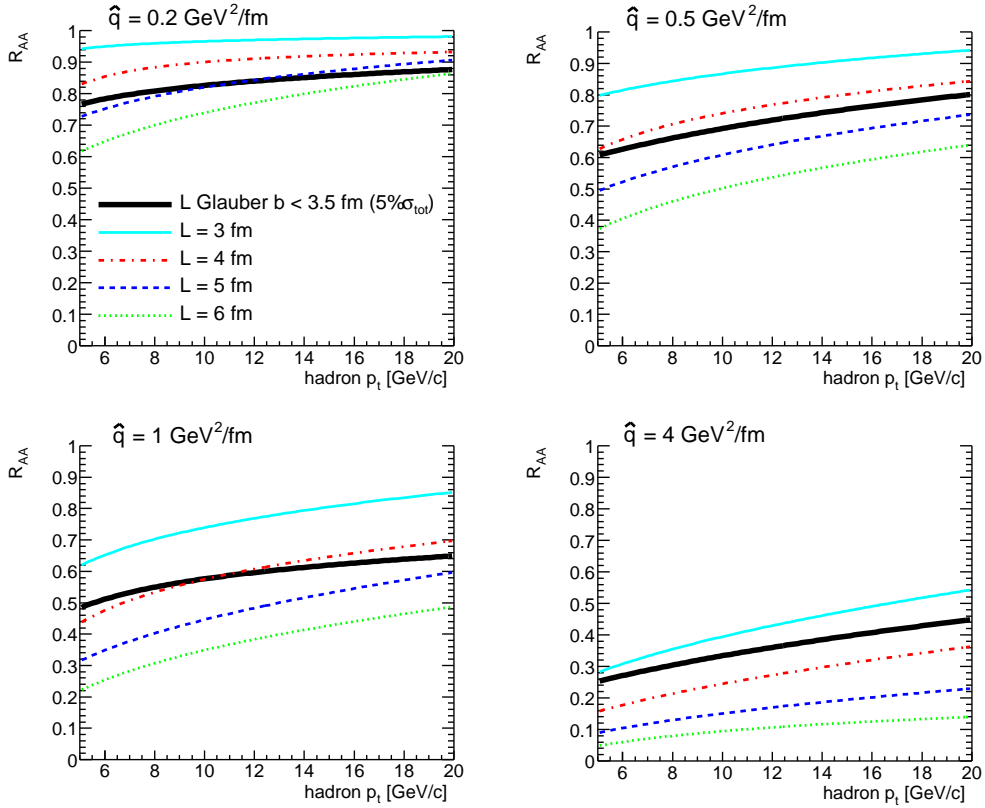


Figure 5: Nuclear modification factor for charged hadrons for different values of  $\hat{q}$  as obtained using the complete Glauber-based distribution (from Fig. 1) or constant values of  $L$ .

at the LHC than at RHIC.

Because of the kinematic constraint  $\Delta E \leq E$ , the use of a constant length of the order of the nuclear radius or even the use of the average length from a detailed distribution can produce quite different results with respect to those obtained taking into account the complete distribution. This is demonstrated in Fig. 5: for  $\hat{q} = 0.5\text{--}1 \text{ GeV}^2/\text{fm}$ ,  $L = 6 \text{ fm}$  gives almost a factor 2 difference in  $R_{AA}$  at  $p_t \sim 10 \text{ GeV}/c$  and the complete  $L$  distribution is equivalent to a constant length which decreases as  $\hat{q}$  increases, 5, 4.5, 4, 3.5 fm for  $\hat{q} = 0.2, 0.5, 1, 4 \text{ GeV}^2/\text{fm}$ . This behaviour is clearly due to an upper ‘cut-off’ of the length distribution: large lengths correspond to very high values of  $\Delta E$ , but, since  $\Delta E$  cannot be higher than the initial parton energy  $E$ , large lengths are not ‘fully exploited’; this corresponds to a cut-off; e.g. for many partons of moderate energy a length of 8 fm is equivalent to a length of 4 fm,

because after propagating for 4 fm they have lost all their initial energy. As a consequence, the length distribution corresponds to an average ‘effective’ length lower than its arithmetic average. The cut-off moves towards lower lengths as  $\hat{q}$  increases and, thus, the average effective length decreases. For  $\hat{q} = 4 \text{ GeV}^2/\text{fm}$ , the average effective energy loss is approximately:  $\langle \Delta E_{\text{eff}} \rangle \approx \langle \Delta E \rangle \times \langle L_{\text{eff}} \rangle^2 / \langle L \rangle^2 = \langle \Delta E \rangle \times (3.5/4.5)^2 \approx 0.6 \langle \Delta E \rangle$ .

Another important observation revealed by Fig. 5 is the fact that the use of the complete  $L$  distribution reduces the increase of  $R_{\text{AA}}$  with  $p_t$  (at RHIC,  $R_{\text{AA}}$  is found to be independent of  $p_t$  in the range 4–10 GeV/ $c$  [7]). This happens because higher-energy partons can exploit the large- $L$  tail more than lower-energy partons and, consequently, for them the cut-off is shifted towards larger lengths.

Charm quarks are generated using PYTHIA, tuned in order to reproduce the single-inclusive  $c$  (and  $\bar{c}$ )  $p_t$  distribution predicted by the pQCD program HVQMNR [29] with  $m_c = 1.2 \text{ GeV}$  and factorization and renormalization scales  $\mu_F = \mu_R = 2 m_t \equiv 2 \sqrt{m_c^2 + p_t^2}$  (the details on this tuning can be found in Ref. [30]). In HVQMNR we use the CTEQ 5M parton distribution functions [31] including, for Pb–Pb, the nuclear shadowing effect by means of the EKS98 parameterization [32] and the parton intrinsic transverse momentum broadening as reported in Ref. [30]. With these parameters, the  $c\bar{c}$  production yields at central rapidity in pp collisions at  $\sqrt{s} = 14 \text{ TeV}$  and in central (5%) Pb–Pb collisions at  $\sqrt{s_{\text{NN}}} = 5.5 \text{ TeV}$  are  $dN_{\text{pp}}^{c\bar{c}}/dy = 0.016$  and  $dN_{\text{Pb-Pb}}^{c\bar{c}}/dy = 11.5$ , respectively. The yield given for Pb–Pb already includes a 65% reduction due to shadowing.

Energy loss for charm quarks is simulated following a slightly different procedure with respect to that for light quarks and gluons. Since the total number of  $c\bar{c}$  pairs per event has to be conserved, in the cases where the sampled  $\Delta E$  is larger than  $p_t$ , we assume the  $c$  quark to be thermalized in the medium and we give it a transverse momentum according to the distribution  $dN/dm_t \propto m_t \exp(-m_t/T)$ , as suggested in Ref. [15]. We use  $T = 300 \text{ MeV}$  as the thermalization temperature for  $c$  quarks. The other difference with respect to the case of massless partons is that we use the standard string model in PYTHIA for the  $c$ -quark fragmentation (more details can be found in Ref. [33]).

## 4 Charm reconstruction with ALICE

The transverse momentum distribution of charm mesons produced at central rapidity,  $|y| < 1$ , can be directly measured from the exclusive reconstruction of  $D^0 \rightarrow K^- \pi^+$  (and charge conjugates) in the Inner Tracking System (ITS),

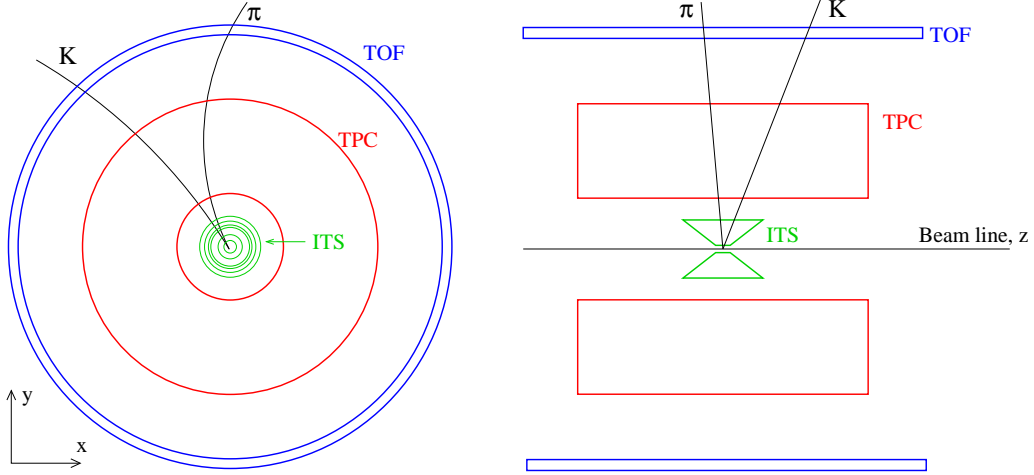


Figure 6: Schematic view of the detectors employed for the reconstruction of  $D^0 \rightarrow K^- \pi^+$  decays in ALICE.

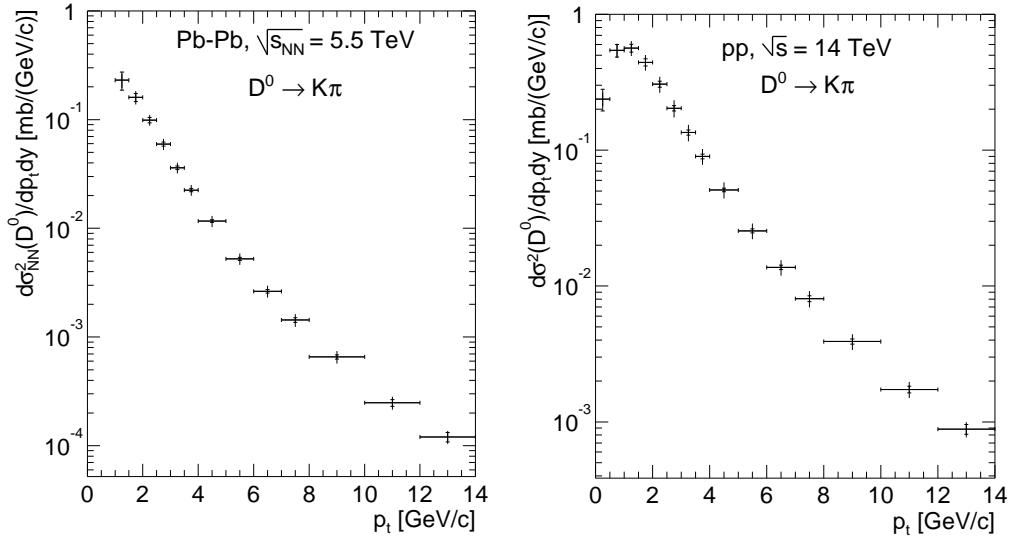


Figure 7: Double-differential cross section per nucleon–nucleon collision for  $D^0$  production as a function of  $p_t$ , as it can be measured with  $10^7$  central Pb–Pb events (left), corresponding to 1-month data-taking, and  $10^9$  pp minimum-bias events (right), corresponding to 9-months data-taking. Statistical (inner bars) and  $p_t$ -dependent systematic errors (outer bars) are shown. A normalization error of 11% for Pb–Pb and 5% for pp is not shown.

Time Projection Chamber (TPC) and Time Of Flight (TOF) of the ALICE barrel ( $|\eta| < 0.9$ ). A schema of the employed detectors is reported in Fig. 6. The displaced vertices of  $D^0$  decays ( $c\tau = 124 \mu\text{m}$ ) can be identified in the ITS with silicon pixels, that provide a measurement of the track impact parameters to the collision vertex with a resolution better than  $50 \mu\text{m}$  for  $p_t > 1 \text{ GeV}/c$ . The low value of the magnetic field (0.4 T) and the  $K/\pi$  separation in the TOF detector allow to extend the measurement of the  $D^0$  production cross section down to almost zero transverse momentum. The strategy for this analysis and the selection cuts to be applied were studied with a realistic and detailed simulation of the detector geometry and response, including the main background sources [33, 34].

The expected performance for central Pb–Pb ( $b < 3.5 \text{ fm}$ ) at  $\sqrt{s_{\text{NN}}} = 5.5 \text{ TeV}$  and pp collisions at  $\sqrt{s} = 14 \text{ TeV}$  is summarized in Fig. 7. The accessible  $p_t$  range is 1–14  $\text{GeV}/c$  for Pb–Pb and 0.5–14  $\text{GeV}/c$  for pp, without assuming dedicated triggers; triggering on high- $p_t$  tracks or on more specific kinematic and topological features using the High Level Trigger may allow to further extend these  $p_t$  ranges. The statistical error corresponding to 1 month of Pb–Pb data-taking and 9 months of pp data-taking is better than 15–20% and the systematic error (acceptance and efficiency corrections, subtraction of the feed-down from  $B \rightarrow D^0 + X$  decays, cross-section normalization, centrality selection for Pb–Pb) is better than 20%. More details are given in Ref. [33].

## 5 Results: $R_{\text{AA}}$ and $R_{\text{D}/h}$

The nuclear modification factor (1) for  $D^0$  mesons is reported in Fig. 8. Nuclear shadowing, parton intrinsic transverse-momentum broadening and energy loss are included. The dead-cone effect is not included in the left-hand panel and included in right-hand panel. Different values of the transport coefficient are used for illustration; we remind that the value expected on the basis of the pion quenching observed at RHIC is  $\hat{q} = 4 \text{ GeV}^2/\text{fm}$ . The reported statistical (bars) and systematic (shaded area) errors are obtained combining the previously-mentioned errors in Pb–Pb and in pp collisions and considering that the contributions due to cross-section normalization, feed-down from beauty decays and, partially, acceptance/efficiency corrections will cancel out in the ratio. An uncertainty of about 5% introduced in the extrapolation of the pp results from 14 TeV to 5.5 TeV by pQCD is also accounted for (see Ref. [33]).

The effect of shadowing, clearly visible for  $\hat{q} = 0$  (no energy loss) as a suppression of  $R_{\text{AA}}$ , is limited to  $p_t < 6\text{--}7 \text{ GeV}/c$  (using EKS98 [32]). Above

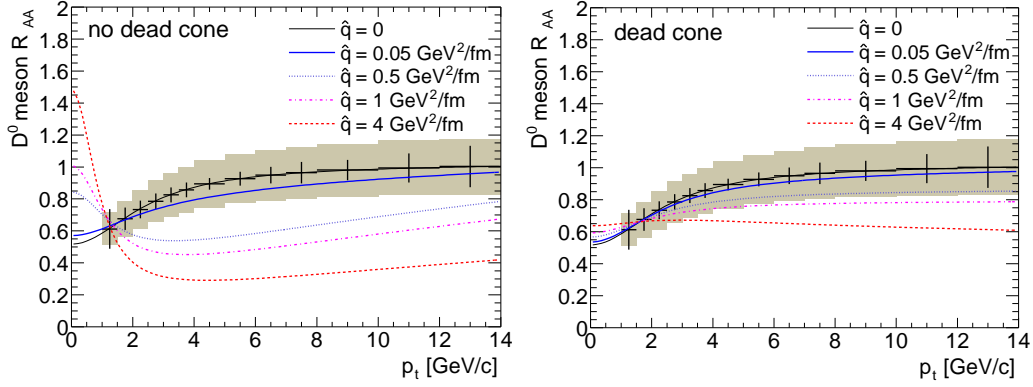


Figure 8: Nuclear modification factor for  $D^0$  mesons with shadowing, intrinsic  $k_t$  broadening and parton energy loss. Left-hand panel: without dead cone correction; right-hand panel: with dead cone correction. Errors corresponding to the curve for  $\hat{q} = 0$  are shown: bars = statistical, shaded area = systematic.

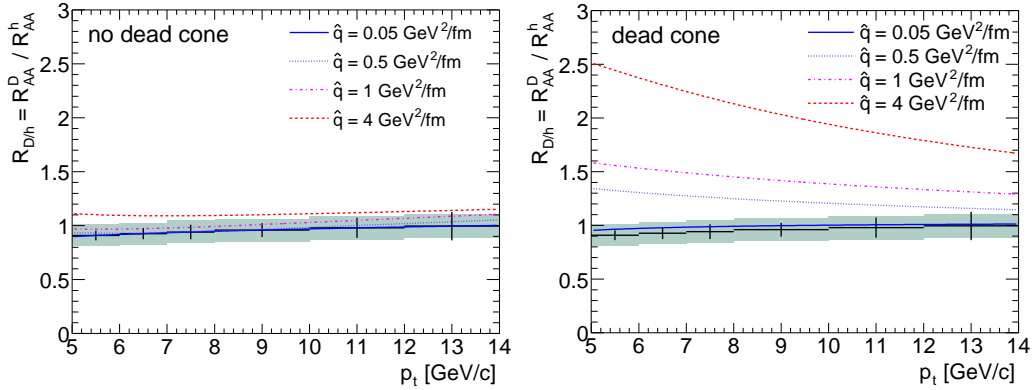


Figure 9: Ratio of the nuclear modification factors for  $D^0$  mesons and for charged hadrons. Left-hand panel: without dead cone correction; right-hand panel: with dead cone correction. Errors corresponding to the curve for  $\hat{q} = 0.05 \text{ GeV}^2/\text{fm}$  are shown: bars = statistical, shaded area = systematic.

this region, only possible parton energy loss is expected to affect the nuclear modification factor of D mesons.

For  $\hat{q} = 4 \text{ GeV}^2/\text{fm}$  and no dead cone, we find  $R_{AA}$  reduced, with respect to 1, by a factor about 3 and slightly increasing with  $p_t$ , from 0.3 at 6  $\text{GeV}/c$  to 0.4 at 14  $\text{GeV}/c$ . Even for a transport coefficient lower by a factor 4,  $\hat{q} = 1 \text{ GeV}^2/\text{fm}$ ,  $R_{AA}$  is significantly reduced (0.5–0.6). When the dead-cone

effect is taken into account, the  $R_{AA}$  reduction due to quenching is found to be lower by about a factor 1.5–2.5, depending on  $\hat{q}$  and  $p_t$ . For our reference transport coefficient, 4 GeV<sup>2</sup>/fm,  $R_{AA}$  with dead cone is equal to 0.6 and essentially flat as a function of  $p_t$ .

We point out that the estimated systematic uncertainty of about 18% may prevent from discriminating between a scenario with moderate quenching and negligible dead-cone effect (e.g.  $\hat{q} = 1$  GeV<sup>2</sup>/fm in the left-hand panel of Fig. 8) and a scenario with large quenching but also strong dead-cone effect (e.g.  $\hat{q} = 4$  GeV<sup>2</sup>/fm in the right-hand panel).

The comparison of the quenching of charm-quark-originated mesons and massless-parton-originated hadrons will be the best-suited tool to disentangle the relative importance of energy-loss and dead-cone effects. The *D/charged hadrons* ratio  $R_{D/h}$ , defined as in (2), is presented in Fig. 9 for the range  $5 < p_t < 14$  GeV/*c*. We used  $R_{AA}^h$  calculated as previously described and  $R_{AA}^{D^0}$ , without and with dead cone, as reported in Fig. 8. Being essentially a double ratio Pb–Pb/Pb–Pb  $\times$  pp/pp, many of the systematic uncertainties on  $R_{D/h}$  cancel out (centrality selection and, partially, acceptance/efficiency corrections and energy extrapolation by pQCD). The residual systematic error is estimated to be of about 10–11%.

We find that, if the dead-cone correction for c quarks is not included,  $R_{D/h}$  is essentially 1 in the considered  $p_t$  range, independently of the value of the transport coefficient, i.e. of the magnitude of the energy-loss effect. When the dead cone is taken into account,  $R_{D/h}$  is enhanced of a factor strongly dependent on the transport coefficient of the medium: e.g. 2–2.5 for  $\hat{q} = 4$  GeV<sup>2</sup>/fm and 1.5 for  $\hat{q} = 1$  GeV<sup>2</sup>/fm. The enhancement is decreasing with  $p_t$ , as expected (the c-quark mass becomes negligible).

The  $R_{D/h}$  ratio is, therefore, found to be enhanced, with respect to 1, only by the dead cone and, consequently, it appears as a very clean tool to investigate and quantify this effect.

Since hadrons come mainly from gluons while D mesons come from (c) quarks, the D/*h* ratio should, in principle, be enhanced also in absence of dead-cone effect, as a consequence of the larger energy loss of gluons with respect to quarks. Such enhancement is essentially not observed in the obtained  $R_{D/h}$  because it is ‘compensated’ by the harder fragmentation of charm quarks with respect to light quarks and, particularly, gluons. With  $z$  the typical momentum fraction taken by the hadron in the fragmentation,  $p_t^{\text{hadron}} = z p_t^{\text{parton}}$ , and  $\Delta E$  the average energy loss for the parton,  $(p_t^{\text{parton}})' = p_t^{\text{parton}} - \Delta E$ , we have

$$(p_t^{\text{hadron}})' = p_t^{\text{hadron}} - z \Delta E, \quad (8)$$

meaning that the energy loss observed in the nuclear modification factor is,

indeed,  $z \Delta E$ . We have, thus, to compare  $z_{c \rightarrow D} \Delta E_c$  to  $z_{\text{gluon} \rightarrow \text{hadron}} \Delta E_{\text{gluon}}$ . With  $z_{\text{gluon} \rightarrow \text{hadron}} \approx 0.4$ ,  $z_{c \rightarrow D} \approx 0.8$  for  $p_t^{\text{D},h} > 5 \text{ GeV}/c$  and  $\Delta E_c = \Delta E_{\text{gluon}}/2.25$  (without dead cone), we obtain

$$z_{c \rightarrow D} \Delta E_c \approx 0.9 z_{\text{gluon} \rightarrow \text{hadron}} \Delta E_{\text{gluon}}. \quad (9)$$

This simple estimate confirms that the quenching for D mesons is almost the same as for (non-charm) hadrons, if the dead-cone effect is not considered.

The errors reported in Fig. 9 show that ALICE is expected to have good capabilities for the study of  $R_{D/h}$ : in the range  $5 < p_t < 10 \text{ GeV}/c$  the enhancement due to the dead cone is an effect of more than  $3 \sigma$  for  $\hat{q} > 1 \text{ GeV}^2/\text{fm}$ . The comparison of the values for the transport coefficient extracted from the nuclear modification factor of charged hadrons and, independently, from the D/*charged hadrons* ratio can provide an important test for the coherence of our understanding of the energy loss of hard probes propagating in the dense QCD medium formed in Pb–Pb collisions at the LHC.

## Acknowledgements

I am grateful to F. Antinori, A. Morsch, G. Paic, E. Quercigh and K. Šafařík (ALICE Collaboration) for comments and suggestions. I enjoyed the many fruitful and stimulating discussions with N. Armesto, K.J. Eskola, C.A. Salgado and U.A. Wiedemann on the phenomenology of parton energy loss.

## References

- [1] ALICE Technical Proposal, CERN/LHCC 95-71 (1995).
- [2] M. Gyulassy and X.N. Wang, Nucl. Phys. **B420** (1994) 583 [arXiv:nucl-th/9306003].
- [3] R. Baier, Yu.L. Dokshitzer, A.H. Mueller, S. Peigné and D. Schiff, Nucl. Phys. **B483** (1997) 291 [arXiv:hep-ph/9607355]; ibidem **B484** (1997) 265 [arXiv:hep-ph/9608322].
- [4] B.G. Zakharov, JETP Lett. **63** (1996) 952 [arXiv:hep-ph/9607440].
- [5] U.A. Wiedemann, Nucl. Phys. **B588** (2000) 303 [arXiv:hep-ph/0005129].
- [6] S.S. Adler *et al.*, PHENIX Coll., Phys. Rev. Lett. **91** (2003) 072301 [arXiv:nucl-ex/0306021].

- [7] J. Jia *et al.*, PHENIX Coll., Nucl. Phys. **A715** (2003) 769c [arXiv:nucl-ex/0209029].
- [8] J. Adams *et al.*, STAR Coll., Phys. Rev. Lett. **91** (2003) 172302. [arXiv:nucl-ex/0305015].
- [9] C. Adler *et al.*, STAR Coll., Phys. Rev. Lett. **90** (2003) 082302 [arXiv:nucl-ex/0210033].
- [10] Yu.L. Dokshitzer and D.E. Kharzeev, Phys. Lett. **B519** (2001) 199 [arXiv:hep-ph/0106202].
- [11] C.A. Salgado and U.A. Wiedemann, Phys. Rev. **D68** (2003) 014008 [arXiv:hep-ph/0302184]; <http://csalgado.home.cern.ch/csalgado>
- [12] M. Gyulassy, P. Lévai and I. Vitev, Nucl. Phys. **B571** (2000) 197 [arXiv:hep-ph/9907461]; Phys. Rev. Lett. **85** (2000) 5535 [arXiv:nucl-th/0005032]; Nucl. Phys. **B594** (2001) 371 [arXiv:nucl-th/0006010].
- [13] A. Accardi *et al.*, Hard Probes in Heavy Ion Collisions at the LHC: Jet Physics [arXiv:hep-ph/0310274].
- [14] M.G. Mustafa, D. Pal, D.K. Srivastava and M.H. Thoma, Phys. Lett. **B428** (1998) 234 [arXiv:nucl-th/9711095].
- [15] Z.W. Lin and R. Vogt, Nucl. Phys. **B544** (1999) 339 [arXiv:hep-ph/9808214].
- [16] Yu.L. Dokshitzer, V.A. Khoze and S.I. Troyan, J. Phys. **G17** (1991) 1602.
- [17] K. Adcox *et al.*, PHENIX Coll., Phys. Rev. Lett. **88** (2002) 192303 [arXiv:nucl-ex/0202002].
- [18] M. Djordjevic and M. Gyulassy, Phys. Lett. **B560** (2003) 37 [arXiv:nucl-th/0302069].
- [19] E. Wang, X.N. Wang and B.W. Zhang [arXiv:nucl-th/0309040].
- [20] R. Baier, Yu.L. Dokshitzer, A.H. Mueller and D. Schiff, JHEP **0109** (2001) 033 [arXiv:hep-ph/0106347].
- [21] R.J. Glauber and G. Matthiae, Nucl. Phys. **B21** (1970) 135.
- [22] A. Drees, H. Feng and J. Jia [arXiv:nucl-th/0310044].
- [23] U.A. Wiedemann, Nucl. Phys. **A690** (2001) 731 [arXiv:hep-ph/0008241].

- [24] K.J. Eskola, H. Honkanen, C.A. Salgado and U.A. Wiedemann, work in progress.
- [25] T. Sjöstrand *et al.*, Computer Phys. Commun. **135** (2001) 238 [arXiv:hep-ph/0010017].
- [26] H.L. Lai *et al.*, CTEQ Coll., Phys. Rev. **D55** (1997) 1280 [arXiv:hep-ph/9606399].
- [27] B.A. Kniehl, G. Kramer and B. Pötter, Nucl. Phys. **B582** (2000) 514 [arXiv:hep-ph/0010289].
- [28] C.A. Salgado and U.A. Wiedemann, private communication.
- [29] M. Mangano, P. Nason and G. Ridolfi, Nucl. Phys. **B373** (1992) 295.
- [30] N. Carrer and A. Dainese, ALICE Internal Note, ALICE-INT-2003-019 (2003) [arXiv:hep-ph/0311225].
- [31] H.L. Lai *et al.*, CTEQ Coll., Eur. Phys. J. **C12** (2000) 375 [arXiv:hep-ph/9903282].
- [32] K.J. Eskola, V.J. Kolhinen, C.A. Salgado, Eur. Phys. J. **C9** (1999) 61 [arXiv:hep-ph/9807297].
- [33] A. Dainese, Ph.D. Thesis [arXiv:nucl-ex/0311004].
- [34] N. Carrer, A. Dainese and R. Turrisi, J. Phys. **G29** (2003) 575.